

1 **Supplemental Appendix**

2 **Exome sequencing identifies *MCM8* mutation in ovarian failure and**  
3 **chromosomal instability**

4

5 Saleh AlAsiri, Sulman Basit, Michelle A. Wood, Svetlana A. Yatsenko, Elizabeth  
6 P. Jeffries, Urvashi Surti, Deborah M. Ketterer, Sibtain Afzal, Khushnooda  
7 Ramzan, Muhammad Faiyaz-UI Haque, Huaiyang Jiang, Michael A. Trakselis,  
8 and Aleksandar Rajkovic

9

10

## 11 **Supplemental Methods**

12 **Patient Recruitment.** A consanguineous family was recruited from King Khalid  
13 University Hospital (KKUH), Riyadh, Saudi Arabia (Figure 1A). The affected  
14 daughters were born to healthy parents (III-1 and III-2) of Saudi Arabian descent  
15 with no previous significant family history of primary amenorrhea or endocrine  
16 dysfunction. The parents are first cousins. There are a total of 12 children (7  
17 females and 5 males). All affected individuals underwent detailed clinical  
18 investigation. Three affected (IV-1, IV-6, and IV-9) and six unaffected family  
19 members (III-1, III-2, IV-2, IV-3, IV-5, and IV-8) of the family provided peripheral  
20 blood samples. Five family members (IV-1, IV-6, IV-9, III-2, and IV-3) provided  
21 skin fibroblast samples. The study was approved by the Ethical Review  
22 Committee of KKUH. Informed written consent was obtained from all participating  
23 subjects.

24

25 **Fertile Control Population.** Women were recruited at Magee-Womens Hospital.  
26 Samples were obtained and de-identified at the time of recruitment. All control  
27 de-identified samples were from Caucasian women who have had at least one  
28 live birth or were currently pregnant with their first child at time of consent. The  
29 study was approved by the Institutional Review Board of the University of  
30 Pittsburgh.

31

32 **DNA Extraction.** Genomic DNA was extracted from peripheral blood samples  
33 using NucleoSpin<sup>®</sup> blood genomic DNA extraction kit (MACHEREY-NAGEL). In a  
34 1.5 ml microcentrifuge tube (Eppendorf AG), 25 µl proteinase K, 200 µl blood and

35 200 µl buffer B3 (NucleoSpin<sup>®</sup>, MACHEREY-NAGEL) were added. The mixture  
36 was vortexed thoroughly for 10-20 seconds and incubated at 70°C for 10-15  
37 minutes followed by addition of 210 µl of ethanol (96-100%) to lysate. The entire  
38 lysate was transferred to a NucleoSpin<sup>®</sup> blood column placed in a collection tube  
39 and centrifuged at 11,000 rpm for 1 minute. The collection tube with flow through  
40 was discarded and the column was placed into a new collection tube. Buffer BW  
41 (500 µl; NucleoSpin<sup>®</sup>, MACHEREY-NAGEL) was added to the column and  
42 centrifuged at 11,000 rpm for 1 minute. Again, the collection tube with flow  
43 through was discarded and the column was placed into a new collection tube.  
44 Buffer B5 (600 µl) was added to the column and centrifuged at 11,000 rpm for 1  
45 minute. The flow-through was discarded and column was dried and placed into a  
46 new 1.5 ml microcentrifuge tube. Preheated (70°C) buffer BE (100 µl) was added  
47 to the column and incubated at room temperature for 1 minute followed by  
48 centrifugation at 11,000 rpm for 1 minute to elute the DNA. Prior to DNA  
49 extraction, the blood collected in the EDTA tubes was equilibrated to room  
50 temperature.

51

52 ***SNP Arrays and Homozygosity Mapping.*** DNA of eight individuals (III-1, III-2,  
53 IV-1, IV-2, IV-3, IV-5, IV-6, and IV-9) was used for homozygosity mapping.  
54 Genotyping was performed using the Affymetrix GeneChip Human Mapping  
55 250K Nsp array (Affymetrix). Data was deposited in the Gene Expression  
56 Omnibus (Accession Number GSE56043). Briefly, 250 ng of genomic DNA was  
57 digested with Digestion Master Mix containing 2 µl NE buffer 2 (10X), 0.5 µl BSA

58 (100X; 10 mg/ml) and 1  $\mu$ l Nsp1. Digested DNA sample was ligated to Nsp1  
59 adaptor using T4 DNA ligase and amplified by 2  $\mu$ l of TITANIUM Taq DNA  
60 polymerase (50X) and 100  $\mu$ M PCR primer. PCR products were purified on a  
61 Clean-Up plate (Clontech Lab) and eluted by RB buffer. Purified PCR products  
62 were fragmented using Fragmentation Reagent (0.05U/ $\mu$ l DNase 1) for 35  
63 minutes at 37°C followed by labeling of fragmented samples with Labeling  
64 Master Mix (30 mM GeneChip<sup>®</sup> DNA Labeling Reagent, 30 U/ $\mu$ l Terminal  
65 Deoxynucleotidyl Transferase) for 4 hours at 37°C. Labeled samples were  
66 hybridized to GeneChip<sup>®</sup> Human Mapping 250K Nsp Array by mixing the sample  
67 with Hybridization Master Mix, denatured on thermoblock and loaded onto the  
68 Array. Array was then placed in a hybridization oven (GeneChip<sup>®</sup> Hybridization  
69 Oven 640) for 16-18 hours. After hybridization, array was washed and stained on  
70 an automated Fluidic Station 450 followed by scanning on GeneChip<sup>®</sup> Scanner  
71 3000 7G using GeneChip<sup>®</sup> Operating Software (GCOS). The genotype of each  
72 SNP was determined by the BRLMM algorithm incorporated in Affymetrix  
73 Genotyping Console. A call rate (percentage of SNPs genotyped by sample) of  
74 98% was obtained across the entire sample. Mapping order, and physical and  
75 genetic distances of SNPs were obtained from Affymetrix. Analysis of SNP data  
76 was conducted using HomozygosityMapper  
77 (<http://www.homozygositymapper.org>). Parametric two point and multipoint  
78 linkage analysis was carried out with the online version of Superlink software.  
79 LOD scores were calculated using a fully penetrant autosomal recessive model

80 with a disease allele frequency of 0.01. Regions of homozygosity with LOD  
81 scores are listed in Supplemental Table 2.

82

83 **Library Construction and Exome Sequencing.** Genomic DNA samples (III-1,  
84 III-2, IV-1, IV-2, IV-3, IV-5, IV-6, and IV-9) were subjected to in-solution exome  
85 enrichment via the HaloPlex Exome Kit (Agilent). Following exome capture, the  
86 samples were submitted for 2 x 100 bp paired end high-throughput sequencing  
87 on a HiSeq 2500 (Illumina, Inc.). Samples were run two samples per flow cell  
88 lane. An average of 14 GB of compressed data and an average of 153,937,273  
89 reads were generated for each sample. Quality metrics for sequencing are  
90 shown in Supplemental Table 6. Raw data were deposited in the Sequencing  
91 Reads Archive (NCBI; ID number SRP046742).

92

93 **Data Alignment and Variant Calling:** Reads were prepared for analysis using  
94 Cutadapt version 1.2.1 to remove the adapters and the Fastx Toolkit 0.0.13.2 to  
95 trim the first 5 bp at 5' end of reads. Data was aligned to GRCh37/hg 19 using  
96 BWA version 0.7.3a MEM (Maximum Exactly Match)<sup>9, 10</sup>. Alignment statistics are  
97 presented in Supplemental Tables 6 and 7. Local realignment around insertions  
98 and deletions, reads base quality recalibration, and variant calling was conducted  
99 using GATK Tool Kits version 2.6-5. GATK HaplotypeCaller (HC) was used to  
100 call variants. The GATK Variant Recalibrator was used to count the VQSLOD  
101 (log odds ratio of variant quality score) based on variants present in the HapMap  
102 (v3.3), 1000 Genomes (Omni2.5 and Gold Standard Indels b37), and dbSNP137

103 databases. Variants were filtered for quality using the following parameters  
104 (Supplemental Table 7): (1) mapping quality filter equal to PASS; (2) Quality  
105 Depth (QD) >2; (3) VQSLOD>0; (4) Mapping Quality (MQ) > 40; (5) Fisher test of  
106 strand bias (FS) < 60; (6) HaplotypeScore < 13; (7) MQRankSum > -12.5; and (8)  
107 ReadPosRankSum > -8. Variants were further filtered if coverage < 10, if the  
108 alternative allele was not called in < 4 reads, if Genotype Quality (GQ) < 5, if the  
109 Polymorphism Likelihood (PL) value >30. Variants were then filtered according to  
110 the Mendelian rule for homozygous recessive inheritance: (1) affected daughters  
111 are homozygous alternative genotype, (2) the parents are heterozygous, and (3)  
112 the unaffected siblings do not have a homozygous alternative genotype.  
113 Remaining variants were annotated using ANNOVAR (Last Change Date: 2013-  
114 02-11) and focus was placed on variants causing non-synonymous variants (in  
115 exons or splice sites) with an allele frequency <5% as reported available  
116 databases (1000 Genomes or the ESP6500 from NHLBI)<sup>11</sup>. Variants were  
117 removed if they appeared on the NIH list of highly polymorphic and frequently  
118 mutated gene lists<sup>12, 13</sup>. Two variants remained.

119

120 **Homology Modeling.** Local and global sequence alignments were performed  
121 using ClustalW2 analysis  
122 (<http://www.ncbi.nlm.nih.gov/blast/bl2seq/wblast2.cgi>). The homology model of  
123 human MCM8 was created by threading the adjusted alignment (WT or P149R)  
124 onto the structure of *Sulfolobus solfataricus* MCM (PDBID: 3F9V<sup>14</sup>) using  
125 SWISS-MODEL<sup>15</sup>. Results are shown in Figure 1C and Supplemental Figure 3.

126

127 **Sanger Sequencing.** Validation of the *MCM8* c.446C>G variant was completed  
128 via PCR amplification of the region surrounding the variant using KAPA HiFi Taq  
129 Polymerase according to manufacturer's instructions. Primers were designed to  
130 amplify genomic region chr20:5,935,793-5,936,051, NCBI37/hg19 (F: 5'-CTG  
131 ACA GAA GGT GGT GAA GTA ACT A; R: 5'-CTC AGT TCT AGC CAA CAT  
132 CTT TTC G). The size of PCR products were confirmed on a 1.5% agarose gel.  
133 PCR products were then sent to Beckman Coulter Genomics for sequencing.  
134 Results were analyzed using Sequencher (Gene Codes Corporation). Samples  
135 for all family members and 200 fertile controls were analyzed. Sample  
136 chromatograms are shown in Figure 1B.

137

138 **Chromosomal Instability Studies.** Peripheral lymphocytes and skin fibroblasts  
139 samples were cultured in the presence of mitomycin C (MMC) or diepoxybutane  
140 (DEB) as described previously<sup>16</sup>. Briefly, cells were cultured in the presence of  
141 MMC at concentration 0 nM, 50 nM, 150 nM, or 300 nM or DEB. Cells were then  
142 harvested after 72 hours of incubation at 37°C. Cells were either dropped onto  
143 microscope slides (peripheral lymphocytes) or cultured on coverslips (patient  
144 fibroblasts). At least ten metaphase spreads per sample were evaluated under  
145 microscope slide for aberrations. Up to 60 aberrations per cell were counted.  
146 Results are reported in Figure 2D. ANOVA for Single Factor variation was utilized  
147 to determine both the effect of drug concentration within each cell line and the  
148 effect of cell line within each drug concentration. Two-tailed T-tests assuming

149 unequal variance were used to compare two cell lines at a single drug  
150 concentration.

151

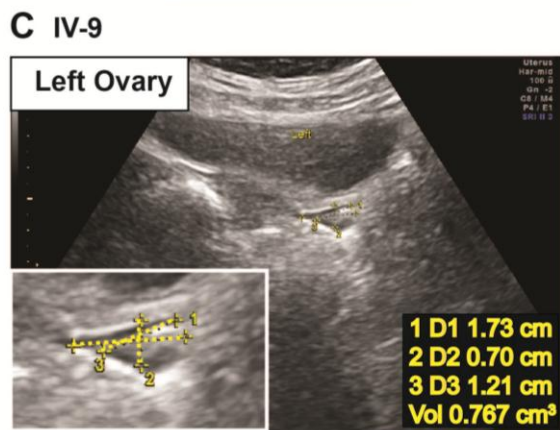
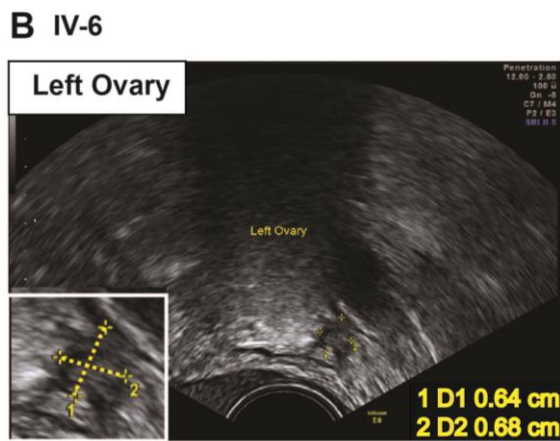
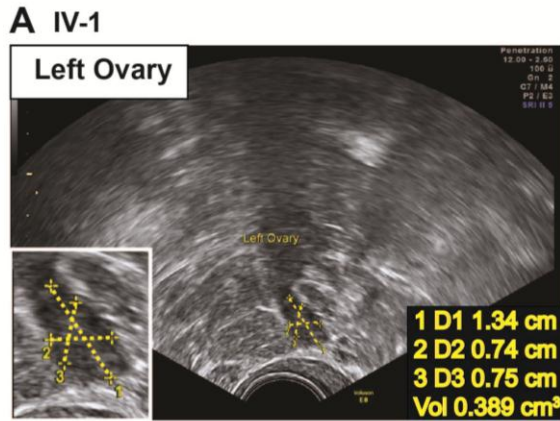
152 **MCM8 Foci Formation Assay.** Human skin keratinocyte (293T) cells were  
153 seeded onto 12-cm glass coverslips coated in poly-L-lysine and cultured in  
154 Dulbecco's Modified Eagle Medium supplemented with 4.5 g/L D-glucose, 4.5 g/L  
155 l-glutamine, 4.5 g/L sodium pyruvate and 10% fetal bovine serum in a humidified  
156 5% CO<sub>2</sub> incubator at 37°C. Human wild-type MCM8 was cloned into pEGFPC2  
157 (Clontech) in frame with the N-terminal GFP tag using *BglIII* and *BamHI*.  
158 pEGFPC2-MCM8 P149R was generated by Quikchange and KAPA HiFi  
159 polymerase introducing an *NruI* site for screening. Transient transfection of  
160 plasmids in 293T cells was performed using Lipofectamine 2000 (Invitrogen)  
161 according to the manufacturer's directions. Cells were incubated with transfection  
162 mixture overnight, before adding 300 nM mitomycin C for 6 hours. Coverslips  
163 were rinsed twice in PBS, incubated in PBS supplemented with 3%  
164 paraformaldehyde for 15 minutes, and then incubated in PBS supplemented with  
165 20% sodium dodecyl sulfate and 10% Triton-X-100 for 15 minutes. Coverslips  
166 were mounted using Fluoroshield + DAPI (Sigma) and imaged using an Olympus  
167 Fluoview 500 or Olyumpus Provis AX70 confocal microscope. GFP foci were  
168 counted in 20 cells per condition. Statistical significance was evaluated by a two-  
169 tailed T-test (assuming unequal variance).

170



171 **MCM8 DNA Binding Assays.** We generated wild-type and mutant MCM8  
172 cDNAs corresponding to the N-terminus of the protein that is predicted to bind  
173 DNA, and compared their ability to bind DNA. The wild type MCM8 cDNA  
174 fragment that encodes N-terminus (nucleotides 1-1104; amino acids 1-368) was  
175 amplified from HeLa cell cDNA with Accuzyme polymerase (Bioline; F: 5'-CAC  
176 CGG ATT CAT GAA TGG AGA GTA TAG AGG CAG; R: 5'- ATT ATG CAT CTA  
177 CTG TCC TTT GCT ATT ACT AAT AGA ATT TG), and subcloned into a pET30a  
178 expression vector (EMD Chemicals) using *BamHI* and *NotI* to allow for  
179 expression of an N-terminal 6XHis tag used in purification. The c.446C>G  
180 mutation was generated using a standard QuikChange protocol with KAPA HiFi  
181 DNA polymerase. MCM8 wild-type and mutant proteins were induced in  
182 BL21(DE3) Rosetta 2 cells with IPTG (0.1 mM; 16 hours at 15°C). Cells were  
183 lysed and sonicated (buffer: 20 mM sodium phosphate buffer [pH 7.5], 300 mM  
184 NaCl, 10 mM imidazole, 10 mM β-mercaptoethanol, and lysozyme). Soluble  
185 protein was purified using a nickel column (Thermo Fisher), washed with 100 mM  
186 NaCl, eluted with 250 mM imidazole, and further purified using an AKTA Prime  
187 FPLC system with a HiTrap heparin column (GE Healthcare). Final cleanup and  
188 sizing was performed with a Superdex 200 26/60 column (GE Healthcare). The  
189 extinction coefficient of MCM8 1-368 was determined to be 40,380 M<sup>-1</sup> cm<sup>-1</sup>.  
190 Electrophoretic mobility shift assays (EMSAs) were performed. As the affinity of  
191 MCM8 to DNA remains unknown, we chose a random 46 nucleotide long single  
192 stranded DNA (ssDNA; 5'-CGA TGA GAG CGA GTC GCA TGG TAT CCC GTA  
193 AAT TGG GAT GCT TAG GCT TA – 3'), as RAD51 is recruited to ssDNA ends at

194 sites of damage and MCM8 is likely to bind at these sites (1). EMSAs were  
195 performed in a 15  $\mu$ l reaction volume containing 20 mM sodium phosphate buffer  
196 (pH 7.5), 100 mM NaCl, 20 mM  $\beta$ -mercaptoethanol and 5 nM DNA probe labeled  
197 at the 5'-end using a standard polynucleotide kinase reaction and  $^{32}$ P- $\gamma$ -ATP, and  
198 the indicated amount of MCM8. Binding reactions were allowed to equilibrate for  
199 5 min followed by directly loading onto a 6% polyacrylamide/TBE gel. Gels were  
200 run for 20 minutes at 13 volts  $\text{cm}^{-1}$  followed by imaging using a Storm  
201 phosphorimager (GE Healthscience). Quantification of the fraction of band shift  
202 was performed using the ImageQuant software (v5.0). Data were fit using  
203 Kaleidagraph (Synergy) to a single site binding model defined by  $\Delta F[MCM8]/K_d +$   
204  $[MCM8]$  where  $F$  is the fraction bound and  $K_d$  is the dissociation constant.  
205



**Supplemental Figure 1.**

**Representative Ultrasounds from**

**Affected Daughters.**

Ultrasound

images from each of the affected

daughters (IV-1 – A; IV-6 – B; IV-9 –

C) reveal small uteri and atrophied

ovaries. (A) As visualized by

transabdominal ultrasound, IV-1 had

a left ovarian volume of 4.2 cm<sup>3</sup> but

the right ovary could not be

visualized. (B) IV-6 had a left

ovarian volume of 2.7 cm<sup>3</sup> but the

right ovary could also not be

visualized via transvaginal

ultrasound. (C) As visualized by

transvaginal ultrasound, IV-9

reveals a pinpoint structures seen in

both adnexae, right side with a

volume of 0.7 cm<sup>3</sup> and left with

225 volume of 0.4 cm<sup>3</sup>, probably the ovaries. Insets show larger views of ovary. Only

226 one ovary is shown in each image. Yellow dashed lines indicate length

227 measured.

228

229 **Supplemental Figure 2. Evolutionary comparison of the selected MCM8**  
 230 **region.** CLUSTAL Omega web site (<http://www.ebi.ac.uk/Tools/msa/>) was used  
 231 to align the sequences from MCM8 proteins in human (*Homo*, NP\_001268449.  
 232 1), mouse (*Mus*, NP\_079952.2), frog (*Xenopus*, NP\_001089437.1) and the  
 233 predicted zebrafish sequence (*Danio*, XP\_002665161.2). p.P149R is found at  
 234 the evolutionary conserved Proline (highlighted in yellow).

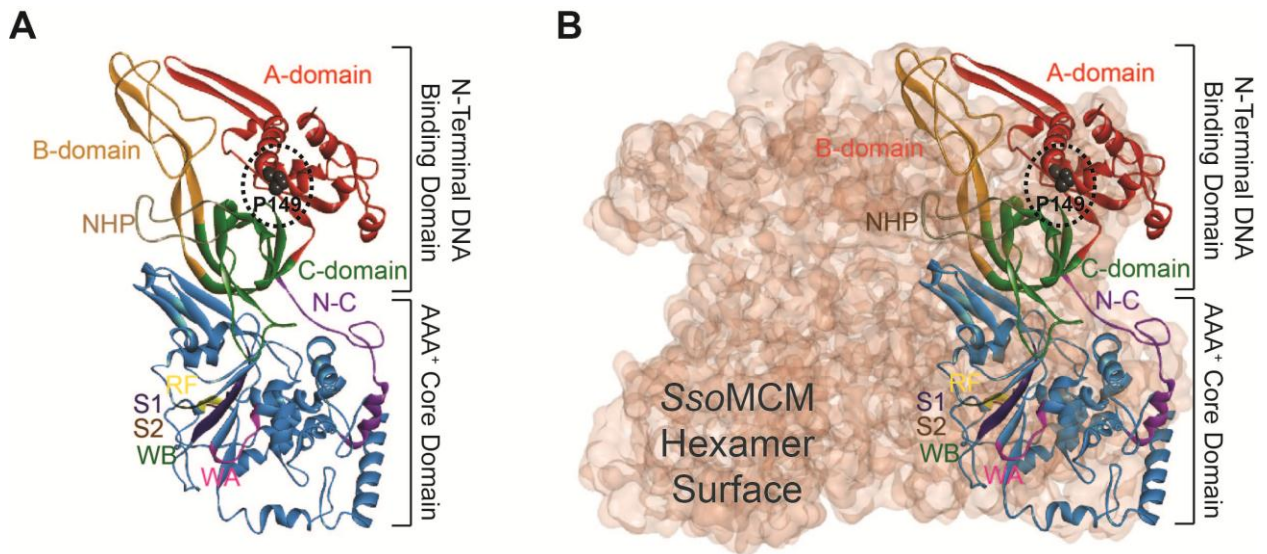
Homo	TSEQTPQ-FLLSTKTPQSMQSTLDRFIPYKGWKLWFSEVYSDSSPLIEKIQAFEKFFTRH	106
Mus	-----ASVYSNNSPFIEKIQAFEKFFTRH	71
Xenopus	NNGRDP--VCFAPPKPQLTQTTLDKYIPYKGWKLWFSEAYSDNSPFLEKVRAFEKFFKKQ	99
Danio	SNNNTQKGNAPQVSQARVTQATLDTTCPYKGWRLYFSEGFEVSSPYVEKIKVFEQYFTSQ	118
	:. :.:.* ** :*:*.**:*. : .	
Homo	IDLYDKDEIERKGSILVDFKELTEGGEVTNLIPIATELRDAP <sup style="background-color: yellow;">E</sup> EKTLACMGLAIHQVLTk	166
Mus	IDLYDKDEIERKGSILVDFKELTKADEITNLIPIENALRDAP <sup style="background-color: yellow;">E</sup> EKTLACMGLAIHQVLTk	131
Xenopus	IELYDKDEIERKGSILVDYKELLQDEDLSAAIP-LSSELKDM <sup style="background-color: yellow;">E</sup> EKVLECMGLAIHQVLTk	158
Danio	IDLYDKDEIERKGSILVDYKDLLSNKQVSHSLPDLARDLKEM <sup style="background-color: yellow;">E</sup> EKILDCLGVAIHQVLTl	178
	*.:*****.****:***. . :.: :* : *.:*** * *.:*****	
Homo	DLERHAAELQAQEGLSNDGETMVNVPHIHARVYNYEPLTQ <sup style="background-color: yellow;">L</sup> KNVRANYYGKYIALRGTVV	226
Mus	DLERHAAELQAQEGLSNGGETMVNVPHIYARVYNYEPLTHLKNIRATCYGKYISIRGTVV	191
Xenopus	DLETHAADLQQQEGLRTEEAPIVNVPFHARVFNYDTLTS <sup style="background-color: yellow;">L</sup> KNLRASLYGKYVALRGTVV	218
Danio	DLERHAAELQGEELPAGIRPIINIPHISARLYNYEPLT <sup style="background-color: yellow;">L</sup> PLKSLRANLYGKFFVIRGTVV	238
	*** **.:** ** * ::*.*. * *:*.*: ** **.:** . **: : :*****	

235  
 236  
 237  
 238

239 **Supplemental Figure 3. Homology Model of human MCM8.** Local and global  
 240 sequence alignments were performed using ClustalW2 analysis  
 241 (<http://www.ncbi.nlm.nih.gov/blast/bl2seq/wblast2.cgi>). The homology model of  
 242 human MCM8 was created by threading the adjusted alignment (WT or P149R)  
 243 onto the structure of *Sulfolobus solfataricus* MCM (PDBID: 3F9V)(2) using  
 244 SWISS-MODEL (3). P149R is located within a loop connecting two alpha-helices  
 245 in the A-domain which pack on top of the C-domain. Proline 149 is circled by a  
 246 black dashed line. NHP - N-terminal hairpin, WA- Walker A, WB - Walker B, S1 -  
 247 Sensor 1, RF - Arginine finger, S2 - Sensor 2, WH - Winged helix. Colored  
 248 domains correspond with linear protein diagram in Figure 1C.

249

250



251

252

**Supplemental Table 1. Clinical Laboratory Investigations of Affected Daughters (IV-1, IV-6, and IV-9).**

	<b>Normal Range<sup>a</sup></b>	<b>IV-1</b>	<b>IV-6</b>	<b>IV-9</b>
FSH (IU/ml)	1.8-22.5 <sup>b</sup>	73.25	95.09	42.13
AMH (ng/ml)	<6.9 <sup>c</sup>	<0.6	<0.6	<0.6
LH (IU/ml)	1.2-100 <sup>b</sup>	22.10	28.93	12.05
Estradiol (pg/ml)	30 to 300 <sup>b</sup>	1.11	10.37	10.82
TSH (mIU/ml)	0.3-5.0 <sup>b</sup>	7.68	6.51	6.24
Prolactin (ng/ml)	3-27	2.5	11.93	14.67
Uterine Volume (cm <sup>3</sup> ) <sup>d</sup>	20-100(4)	18.5	14.6	3.7
Right Ovarian Volume (cm <sup>3</sup> )	6.6±0.19(5)	Not visualized	Not visualized	0.7
Left Ovarian Volume (cm <sup>3</sup> )	6.6±0.19(5)	4.3	2.7	0.4
Anti-Thyroid Antibodies	Negative	Negative	Negative	Negative
Karyotype	46,XX	46,XX	46,XX	46,XX

<sup>a</sup>All hormone measures provided were prior to hormone replacement therapy.

<sup>b</sup>Mayo Clinic, Mayo Medical Laboratories, Rochester, MN.

<sup>c</sup>Reference Range for Adult Females, Esoterix Lab, Calabasas, CA.

<sup>d</sup>Uterine volume calculated by using the formula for prolate ellipsoid: longitudinal diameter x anterioposterior diameter x transverse diameter x 0.5233. Range based on Tanner stage 4-5 or adult uterine volumes.

253

254

255

<b>Supplemental Table 2: Regions of Homozygosity Based on SNP Array</b>			
<b>Chromosome</b>	<b>Coordinates (hg19)</b>	<b>Siblings in Which Region Identified</b>	<b>LOD Score</b>
Chr 1	2010994-4953528	Unaffected and Affected	1.53
Chr 12	81229423-82251957	Unaffected and Affected	-0.65
Chr 19	21157697-28750407	Unaffected and Affected	0.66
Chr 20	65288-1136217	Affected Only	1.58
Chr 20	2163414-4313037	Affected Only	1.18
Chr 20	4861939-6976715	Affected Only	2.77

256  
257

<b>Supplemental Table 3. Chromosomal Breakage as Induced by DEB treatment in Patient Lymphocytes (Raw Data).</b>			
	<b>Patient</b>		
<b>Cell Number</b>	<b>Control</b>	<b>IV-1</b>	<b>IV-6</b>
1	0	0	0
2	0	1	0
3	0	0	0
4	1	0	0
5	0	0	0
6	0	0	0
7	0	0	0
8	0	0	0
9	0	0	0
10	0	0	0
Total Number of Breaks	1	1	0
Average Number of Breaks Per Cell	0.1	0.1	0

258



**Supplemental Table 4. WES Variants in Genes Known to Be Involved in Chromosomal Instability or Primary Amenorrhea.**

<b>Gene</b>	<b>Associated Syndrome</b>	<b>Variant</b>
<i>ATM</i>	Ataxia-telangiectasia	Benign SNP
<i>BRCA1</i>	Breast Cancer	Benign SNP
<i>BRCA2</i>	Fanconi Anemia, Wilms tumor, and cancers	Benign SNP
<i>BRIP1</i>	Fanconi anemia, Breast Cancer	Benign SNP
<i>ERCC4</i>	Fanconi anemia	None
<i>FANCA</i>	Fanconi anemia	None
<i>FANCB</i>	Fanconi anemia	None
<i>FANCC</i>	Fanconi anemia	None
<i>FANCD2</i>	Fanconi anemia	None
<i>FANCE</i>	Fanconi anemia	None
<i>FANCF</i>	Fanconi anemia	None
<i>FANCM</i>	Fanconi anemia	None
<i>FMR1</i>	Fanconi anemia	None
<i>HGPS</i>	Hutchinson-Gilford progeria	None
<i>MLH1</i>	Mismatch repair cancer syndrome	None
<i>MLH3</i>	Colorectal Cancer, Endometrial Cancer	Benign SNP
<i>MSH2</i>	Mismatch repair cancer syndrome	None
<i>MSH3</i>	Endometrial carcinoma	Benign SNP
<i>MSH6</i>	Mismatch repair cancer syndrome	Benign SNP
<i>NBN</i>	Nijmegen breakage syndrome	Benign SNP
<i>NBS1</i>	Nijmegen Breakage Syndrome	None
<i>PALB2</i>	Fanconi anemia	None
<i>PHF9</i>	Fanconi anemia	None
<i>RAD50</i>	Nijmegen breakage syndrome-like disorder	None
<i>RAD51C</i>	Fanconi anemia	None
<i>SLX4</i>	Fanconi anemia	None
<i>TP53</i>	Multiple Cancers	Benign SNP
<i>WRN</i>	Werner syndrome	Benign SNP
<i>XPC</i>	Xeroderma pigmentosum	Benign SNP
<i>XRCC9</i>	Fanconi anemia	None

259

260

261

<b>Supplemental Table 5. Quality Metrics for Sequencing by Sample.</b>								
<b>Lane on Flow Cell</b>	<b>Sample ID</b>	<b>Yield (Mbases)</b>	<b>Number of Reads</b>	<b>% of raw clusters per lane</b>	<b>% of Perfect Index Reads</b>	<b>% of One Mismatch Reads (Index)</b>	<b>% of <math>\geq</math> Q30 Bases (PF)</b>	<b>Mean Quality Score (PF)</b>
1	IV-9	14,038	140,381,192	44.02	98.8	1.2	89.87	35.09
1	IV-6	17,497	174,966,244	54.86	98.78	1.22	89.41	34.95
2	IV-1	9,115	91,146,660	33.77	84.25	15.75	91.5	35.57
2	IV-5	17,302	173,024,000	64.1	84.3	15.7	91.34	35.52
3	IV-3	15,629	156,291,636	45.32	86.61	13.39	88.3	34.64
3	III-1	18,405	184,050,526	53.37	86.76	13.24	88.06	34.57
4	III-2	16,120	161,199,806	48.58	99.35	0.65	89.69	35.04

262

263

<b>Supplemental Table 6. Exome Sequencing Alignment Statistics by Sample.</b>				
<b>Sample ID</b>	<b>Reads Aligned to the Exome</b>	<b>Average Coverage Across Exome</b>	<b>Reads Aligned to Targeted Capture Region</b>	<b>Average Coverage Across Capture Region</b>
IV-9	119,310,892	185	135,472,892	108
IV-6	147,764,231	233	169,010,803	137
IV-1	77,587,856	122	88,188,326	71
IV-5	147,215,164	230	166,322,091	133
IV-3	132,631,196	208	151,363,205	122
III-1	155,921,867	244	177,658,272	143
III-2	136,878,377	214	155,104,064	125

264  
265

**Supplemental Table 7. Variant Filtration for Homozygous Recessive Inheritance Pattern.**

	<b>Variants Remaining</b>
Total Variants Called in the Family	120,201
Application of GATK Quality Filters, variant kept if: (1) mapping quality filter = PASS (2) Quality Depth (QD) >2 (3) VQSLOD>0 <sup>a</sup> (4) Mapping Quality (MQ) > 40 (5) Fisher test of strand bias (FS) < 60 (6) HaplotypeScore < 13 (7) MQRankSum > -12.5 (8) ReadPosRankSum > -8 (9) coverage > 10 (10) alternative allele called in > 4 reads (11) Genotype Quality (GQ) > 5, (12) Polymorphism Likelihood (PL) value difference <30	86,135
Application of Homozygous Recessive Inheritance Model: (1) affected daughters are homozygous alternative genotype (2) parents are heterozygous (3) unaffected siblings do not have a homozygous alternative genotype	1,030
Variants in Exons or Splice Sites as annotated using ANNOVAR (Last Change Date: 2013-02-11)	630
Nonsynonymous Variants	293
Remove Known Polymorphic Genes from NIH Recommendations (6, 7)	256
Variants with a Minor Allele Frequency <5% as reported in available databases (1000 Genomes and ESP6500 from NHLBI)	2
<sup>a</sup> The GATK Variant Recalibrator was used to count the VQSLOD (log odds ratio of variant quality score) based on variants present in the HapMap (v3.3), 1000 Genomes (Omni2.5 and Gold Standard Indels b37), and dbSNP137 databases.	

## REFERENCES

- 267  
268  
269 1. Park, J., Long, D.T., Lee, K.Y., Abbas, T., Shibata, E., Negishi, M., Luo,  
270 Y., Schimenti, J.C., Gambus, A., Walter, J.C., et al. 2013. The MCM8-  
271 MCM9 complex promotes RAD51 recruitment at DNA damage sites to  
272 facilitate homologous recombination. *Mol Cell Biol* 33:1632-1644.
- 273 2. Brewster, A.S., Wang, G., Yu, X., Greenleaf, W.B., Carazo, J.M., Tjajadi,  
274 M., Klein, M.G., and Chen, X.S. 2008. Crystal structure of a near-full-  
275 length archaeal MCM: functional insights for an AAA+ hexameric helicase.  
276 *Proc Natl Acad Sci U S A* 105:20191-20196.
- 277 3. Arnold, K., Bordoli, L., Kopp, J., and Schwede, T. 2006. The SWISS-  
278 MODEL workspace: a web-based environment for protein structure  
279 homology modelling. *Bioinformatics* 22:195-201.
- 280 4. Holm, K., Laursen, E.M., Brocks, V., and Muller, J. 1995. Pubertal  
281 maturation of the internal genitalia: an ultrasound evaluation of 166  
282 healthy girls. *Ultrasound Obstet Gynecol* 6:175-181.
- 283 5. Pavlik, E.J., DePriest, P.D., Gallion, H.H., Ueland, F.R., Reedy, M.B.,  
284 Kryscio, R.J., and van Nagell, J.R., Jr. 2000. Ovarian volume related to  
285 age. *Gynecol Oncol* 77:410-412.
- 286 6. Fuentes Fajardo, K.V., Adams, D., Program, N.C.S., Mason, C.E., Sincan,  
287 M., Tifft, C., Toro, C., Boerkoel, C.F., Gahl, W., and Markello, T. 2012.  
288 Detecting false-positive signals in exome sequencing. *Hum Mutat* 33:609-  
289 613.

290 7. Adams, D.R., Sincan, M., Fuentes Fajardo, K., Mullikin, J.C., Pierson,  
291 T.M., Toro, C., Boerkoel, C.F., Tifft, C.J., Gahl, W.A., and Markello, T.C.  
292 2012. Analysis of DNA sequence variants detected by high-throughput  
293 sequencing. *Hum Mutat* 33:599-608.  
294  
295